

F. Crisanti, A. Becoulet, P. Buratti, E. Giovannozzi, C. Gormezano, E. Joffrin,
A. Sips, C. Bourdelle, A. Cardinali, C. Challis, N. Hawkes, J. Hobirk,
X. Litaudon, G. Regnoli, M. Romanelli, A. Thyagaraja, A. Tuccillo
and JET EFDA contributors

JET Hybrid Scenarios with Improved Core Confinement

“This document is intended for publication in the open literature. It is made available on the understanding that it may not be further circulated and extracts or references may not be published prior to publication of the original when applicable, or without the consent of the Publications Officer, EFDA, Culham Science Centre, Abingdon, Oxon, OX14 3DB, UK.”

“Enquiries about Copyright and reproduction should be addressed to the Publications Officer, EFDA, Culham Science Centre, Abingdon, Oxon, OX14 3DB, UK.”

JET Hybrid Scenarios with Improved Core Confinement

F. Crisanti¹, A. Becoulet², P. Buratti¹, E. Giovannozzi¹, C. Gormezano¹, E. Joffrin²,
A. Sips¹, C. Bourdelle², A. Cardinali¹, C. Challis⁴, N. Hawkes⁴, J. Hobirk³,
X. Litaudon², G. Regnoli¹, M. Romanelli¹, A. Thyagaraja⁴, A. Tuccillo¹
and JET EFDA contributors*

¹*Associazione Euratom-ENEA sulla Fusione, C.R. Frascati, Frascati, Italy*

²*Association Euratom-CEA, DSM/DRFC, Cadarache F-13108, France*

³*Max-Planck-Institut für Plasmaphysik, Euratom Association, 85748 Garching, Germany*

⁴*Euratom/UKAEA Fusion Association, Culham Science Centre, Abingdon, Oxon, OX14 3DB, UK*

* *See annex of M. L. Watkins et al, "Overview of JET Results",
(Proc. 21st IAEA Fusion Energy Conference, Chengdu, China (2006)).*

Preprint of Paper to be submitted for publication in Proceedings of the
21st IAEA Fusion Energy Conference,
(Chengdu, China, 16th October - 22nd October 2006)

ABSTRACT.

The data from the Hybrid scenario experiments has been incorporated into a large database that contains more than 40 plasma and scenario parameters. Analysis of the database has revealed that there is a spectrum of temperature gradient scale lengths that exceed the critical level considered at JET to indicate the presence of an ITB. In the best example ($B_T = 2.5\text{T}$, $I_p = 2.1\text{MA}$, $P_{\text{NBI}} = 13.4\text{MW}$, $P_{\text{ICRH}} = 2.5\text{MW}$, $1 < q(0) < 1.5$) it was $R/(L_{T_i}) \sim 14$ and $R/(L_{T_e}) \sim 11$ in a wide region ($\Delta r \sim 0.2\text{m}$) of the plasma core ($r/a \sim 0.4$). The central ion and electron temperatures were $T_i(0) \sim 17\text{keV}$ and $T_e(0) \sim 8\text{keV}$. In the initial phase of the heating pulse the edge temperatures had been quite low ($T_i \sim T_e \sim 2\text{keV}$), but suddenly they increased to $\sim 4\text{keV}$ while, at the same time, the edge density decreased providing a more or less constant edge pressure. The discharge was essentially without ELMs, although the additional heating power was well above the usual Hmode power threshold. The global performance was comparable to, or slightly better than that of an equivalent standard Hybrid discharge with type I ELMs ($\beta_N \sim 2$, $H_{89} \sim 2.2$). The plasma energy associated with the pedestal was $W_{\text{ped}} \sim 37\%$ in this discharge, whilst the part within the steep gradient region was $W_{\text{core}} \sim 23\%$. Despite the relatively low density the toroidal rotation was only about half that of a typical JET ITB plasma. Nevertheless, the $E \times B$ shearing rate is calculated to be very large. An analysis using the gyrokinetic code, KINEZERO shows that, in the improved confinement region, ITG-TEM wavelength instabilities should be stable. An important factor in the plasmas with improved core confinement appears to be the density, which was higher in the case of similar Hybrid plasmas without core confinement improvement. Transport analysis of discharges with and without core confinement improvement will be presented and compared.

1. INTRODUCTION

Plasma scenarios are being developed with the aim of providing higher normalised plasma pressure, β_N , and/or longer pulse duration compared with the ELMy H-mode envisaged for the reference inductive operation of ITER. These types of scenarios are often referred to as “Advanced Tokamak scenarios” and, normally, this indicates two quite different approaches: the “steady state” and the “Hybrid” scenario. In both of them good performances have been achieved in several machines (DIII-D, AUG, JET, JT-60U), and a quasi steady state high value of the merit parameter $H\beta_N$ has been obtained [1, 2, 3, 4]. The “steady state” approach relies on a region of improved thermal insulation in the core, called an Internal Transport Barrier (ITB) [1,5], to provide high fusion performance and the large self-generated bootstrap current necessary for efficient steady-state operation. In this plasma region the value of minimum q is generally in the range $1.5 \div 2$, whilst the magnetic shear can be negative or close to zero. There is experimental and theoretical evidence that the $E \times B$ shearing rate, as well as the zero and/or negative magnetic shear, can be important factors in suppressing the turbulent transport mechanisms, such as Ion Temperature Gradient (ITG) modes, leading to the formation of such ITBs. Another approach capable of accessing high β_N , called the “Hybrid” scenario [6], relies on maintaining central safety factor, q , just above unity in a large region of low magnetic shear; however, so far, this approach does not aim to address the full Current

Drive operations. This scenario, sometimes called an “Improved H-mode” [7], is often characterized by on a good confinement region at the plasma edge [8], as in a standard Hmode. The main difference, however, comes from the central MHD behaviour in the absence of a $q=1$ region, and consequent avoidance of the sawtooth trigger for large Neoclassical Tearing Modes (NTMs) [9]. An important issue is whether confinement properties of the plasma core in Hybrid scenarios can be significantly improved compared to the ELMy (Edge Localised Mode) H-mode. A significant effort has been devoted to the investigation of Hybrid scenarios on JET [6]. In some experiments, dedicated to compare ASDEX Upgrade and JET, the possibility to get ITBs was investigated in these scenarios [10]. The data from these experiments have been incorporated into a large database. The database analysis will be presented in order to gain an overview of the plasma behaviour under various experimental conditions and highlight the general trends; moreover, a comprehensive analysis of specific pulses will be presented in order to contrast the behaviour of cases with and without an apparent improved core confinement.

2. DATABASE

In the database we have included almost all the Hybrid scenario experiments performed at JET, either with ion dominant heating [6] or with electron dominant heating [11]. The database comprises ≈ 100 discharges and ≈ 280 time points, and contains around 40 plasma and scenario parameters, including some parameters to characterise the edge behaviour like the edge neoclassical collisionality and the ELM frequency. At least two time points for any single discharge have been included, one of them being the time of maximum β_N . In order to minimise the risk of some accidental data fluctuation, a time averaging of 100ms has been done. The largest part of the experiments have been realized at $q_{95} \sim 4$, essentially with three different values of toroidal magnetic field ($B_T = 1.7 - 2.4 - 3.1$ T) and plasma current ($I_p = 1.4 - 2.1 - 2.8$ MA). However, the experiments with dominant electron heating have mainly been performed with $q_{95} \sim 5.5$. A large variation of the total injected power has been studied; in particular it has been largely varied the interplay between the ICRH and the NBI to study situations with mainly ion and/or electron heating. Unfortunately, in this last configuration the ion temperature measurement was not available [11]. Analysis of the database has revealed that there is a spectrum of temperature gradient scale lengths ($6 < R/L_{T_i}$ or $R/L_{T_e} < 15$), which extend to values of $\rho^*_{T_i}$ (the ion Larmor radius at the sound speed normalised to LT) that exceed the critical level considered at JET to indicate the presence of an ITB ($\rho^*_{T_i} = 1.4 \times 10^{-2}$ [12]). This point is highlighted in Fig.1 and Fig.2 where the profile maximum of the parameters $\rho^*_{T_i}$ and R/L_{T_e} are shown versus the merit parameter $H_{89} \leq \beta_N$. The presented data have been selected with the constraint that the maxima of both gradient parameters occur in the plasma region with $3.2 < R < 3.55$ m. The data are reported separated by toroidal field, showing the occurrence of a high temperature gradient region at any value of B_T . A more rough way to highlight this gradient enhancement is to plot the central temperatures $T(0)$ versus the volume averaged temperatures $\langle T \rangle$. For the largest part of the database $T_i(0)/\langle T_i \rangle \sim 2.5$, but it become of the order of 3.3 in the

discharges with the enhanced core confinement. In the performed experiments the electron density has been varied over a wide range ($1.5 < n_e(0) < 8^0 \times 10^{19} \text{ m}^{-3}$). Fig.3 shows the central ion temperatures versus the central electron densities, which can also be used as a merit parameter for the ion energy confinement. It is evident that the improvement of the core confinement (higher T_i) decreases with the increase of the plasma density and that it practically disappears for $n_e(0) > 4.5^0 \times 10^{19} \text{ m}^{-3}$. It is also worth noting that this “threshold” density tends to increase with increasing B_T . Three discharges with similar discharge parameters, with the exception of the density, are also highlighted in Fig.3. It is worth noting that, in the database, the central plasma pressure shows the same behaviour of the central temperature, confirming that the improved core confinement depends on the plasma density. Another peculiar feature, shown by the database, is that $T_i(0)/T_e(0) \sim 2$ for all the JET standard Hybrid scenario experiments, with the NBI as main heating source. Unfortunately, the charge exchange ion temperature measurement was not available during the experimental campaign with dominant ICRH heating; consequently it is not possible to perform exactly the same analysis. However, for a very large fraction of the full database a single value (around half plasma radius) of the ion temperature was available from the crystal spectroscopy diagnostic. Plotting these data versus the central electron temperature shows a linear behaviour for the data of the standard scenario experiments, dominated by the NBI heating; a similar behaviour was not at all present for the data of the experiments with dominant ICRH heating, where the central electron temperature seems to be de-correlated from the ion temperature. Moreover, $T_e(0)/\langle T_e \rangle \sim 1.75$ for the standard Hybrid scenario, but it increases up to $T_e(0)/\langle T_e \rangle \sim 2.5$ for the discharges with more electron heating.

3. DETAILED ANALYSIS FOR A SINGLE DISCHARGE.

One of the best examples of core confinement improvement highlighted by the database analysis is the Pulse No: 59137 ($B_T = 2.55\text{T}$, $I_p = 2.2\text{MA}$, $r^* \sim 5.5^0 \times 10^{-3}$, $P_{\text{NBI}} = 13.4\text{MW}$, $P_{\text{ICRH}} = 2.5\text{MW}$, $n_e^* \sim 0.05$). This discharge was obtained using the standard JET Hybrid scenario operational techniques that leads to a large central plasma region where $1 < q < 1.5$, as confirmed by the MSE (Motional Stark Effect) measurements, used to constrain the equilibrium code EFIT, by the Faraday Rotation measurements and by the absence of any saw-tooth activity. However, some very important differences were present both in the edge and in the plasma bulk behaviour. In the plasma core ($r/a \sim 0.4$) a wide region ($\Delta r \sim 0.2\text{m}$) was characterized by steep electron and ion temperature gradients with normalized inverse gradient scale length ($R/L_{T_i} \sim 14$, $R/L_{T_e} \sim 11$) larger than in standard H-mode. In Fig.4a,b are respectively shown the normalized Larmor radius for the electrons, $r^*_{T_e}$, and for the ions, $r^*_{T_i}$. It is clearly evident that the region with $r^*_{T_i} > 1.4^0 \times 10^{-2}$ is quite large, whilst for the electrons the region with a large temperature gradient is very tiny and very close to the plasma centre. Here it has to be considered that the ion temperature measure has a poorer radial resolution ($\approx 8\text{cm}$). The steep gradient was steady for almost 5 second and, in this experiment, was only limited by the NBI duration. In Fig.5 we show the radial profiles of the electron and ion temperatures (from the Electron Cyclotron Emission and from the Charge- Exchange), of the electron density

(from the Thomson scattering) and of the toroidal rotation (from the Charge-Exchange), at four different times. The times have been selected to show the transition phase to the enhanced central confinement and the highest achieved performance. Also, from a cursory inspection of the temperature profiles, the strong ion temperature gradient and the large involved region are evident. For the electron temperature the gradient increases only slightly, in a more internal plasma region and for a shorter time. The central ion temperature is very high, $T_i(0) \sim 17\text{keV}$, and strongly decoupled from the electrons ($T_e(0) \sim 8\text{keV}$). It has to be noted that the factor two between the electron and ion temperature is equal to the one discussed in the previous paragraph for the standard Hybrid scenario. During the initial part of the heating pulse the edge temperatures were relatively low ($T_i \approx T_e \sim 2\text{keV}$), but in correspondence of a small step-up of the NBI power they increased to $\sim 4\text{keV}$ (around $t = 10.5\text{s}$, see Fig.5); at the same time, the edge density decreased (from ~ 2.8 to $\sim 1.3 \times 10^{19} \text{ m}^{-3}$) providing a more or less constant edge pressure. In fact, there was also a decrease in the central density (from ~ 4.4 to $\sim 3.2 \times 10^{19} \text{ m}^{-3}$) and the density profile remained moderately peaked. It is important to note that, although the additional heating power was well above the usual H-mode power threshold, and even the power normally required to access type I ELMs, for long periods the discharge was essentially without ELM activity. Despite this, the global performance was comparable to, or slightly better than, that of equivalent standard Hybrid discharges with type I ELMs ($\beta_N \sim 2$, $H_{89} \sim 2.2$ and $\beta_N H_{89}/q_{95} \sim 0.3$). Another peculiar feature is that the plasma energy associated with the pedestal was $W_{\text{ped}} \sim 37\%$, comparable with that of a standard H-mode. It is also worth noting that the energy within the steep gradient region was $W_{\text{core}} \sim 23\%$, in spite of the low density and of the small plasma volume involved. Despite the relatively low density in Pulse No: 59137, the toroidal rotation ($\omega_T \sim 1.2 \times 10^5 \text{ rad/s}$) was only about half that of a typical JET ITB plasma and with a quite moderate and constant gradient along the profile (Fig.5). Nevertheless, the $E \times B$ shearing rate is calculated to be large ($\omega_{E \times B} \sim 1.5 \times 10^5 \text{ s}^{-1}$), assuming the poloidal rotation to be neoclassical (although this assumption has recently been called into question [13]). Analysis using the gyrokinetic code, KINEZERO, shows that, in the improved confinement region, instabilities with $k_{\theta} \rho_i < 2$ (ITG-TEM) are foreseen to be stable, although some residual fluctuation remains driven by the trapped electrons.

4. TRANSPORT COMPARISON OF SIMILAR DISCHARGES.

As shown in Fig.3, three discharges have been selected (Pulse No's: 59137, 60933, 62459) with all operational parameter, except the density, relatively similar. The first thing to be noted is that at the three different densities of the compared discharges corresponds a quite different contribution of the non-thermal particles to the energy content. For the Pulse No: 59137 experiment, with improved core confinement and the lowest electron density, around 40% of the total energy is due to the contribution of the fast ion population. This large contribution has been independently evaluated by using the PION code and by comparing the measured diamagnetic energy with the volume integral of the temperature and density measurements. This contribution decreases to around 30% for the intermediate density pulse (Pulse No: 60933) and collapses to $\sim 10\%$ for the discharge with the

highest density. The presence of this large fast ion population, in the discharge with the better core confinement, suggests that this population can play a fundamental role for turbulent transport reduction with a similar mechanism to the one postulated for ASDEX Upgrade [14]. An interpretative transport analysis has been performed using the JETTO for the three compared discharges. The total coupled power to the electrons and to the ions is more or less the same for the three cases. However, the fraction of power that goes to the ion species ($8 \div 10\text{MW}$) is somewhat larger than the one absorbed by the electrons ($4.5 \div 6.5\text{MW}$). In the three pulses the power deposition profile has, more or less, the same peaking factor; however, in the low density discharge, the power is coupled at a larger radius than in the others ($\rho \sim 0.35$, instead of $\rho \sim 0.2$). The analysis shows a sharp decrease of χ_i and a weaker one for χ_e over the entire plasma core region for Pulse No: 59137. For the ion species the radial profile of the heat diffusion coefficient clearly correlates with the macroscopic performance of the three pulses. This can be seen in Fig.6 where χ_i is shown versus time for the three discharges at two fixed normalised plasma radii: $\rho = 0.3$ and $\rho = 0.7$. In the core region $\langle i$ is smaller for the discharge with the lowest central plasma density and with the largest central ion and electron temperature. In the other two pulses, by increasing the central density $\langle i$ increases as well. Exactly the opposite behaviour can be noticed in the external region of the plasma, indicating the better pedestal property of the discharges with higher density. JETTO has also been used to evaluate the fraction of non-inductive driven plasma current. In order to check the results of the analysis, it has been controlled that the simulated JETTO loop voltages reproduce well the experimental measurements. The analysis has shown that the total bootstrap current has a slight variation among the three discharges, varying from a fraction of $\sim 30\%$ for the discharge at highest density and decreasing, respectively, down to $\sim 25\%$ and $\sim 20\%$ with the decrease of the density. However the total non-inductive current is more or less of the same order for all the pulses ($\sim 35\%$) as a consequence of an opposite behaviour of the current driven by the NBI.

5. PLASMA EDGE CHARACTERIZATION.

An important point to note is the completely different ELM behaviour in the three discharges compared above. As was already mentioned, the Pulse No: 59137, with the improved core confinement, has practically no ELM activity, although the total injected power is well above the type I ELM threshold. By increasing the density the ELM behaviour changes drastically and, in the Pulse No: 62459 strong type I ELM activity is present. In order to get a better characterization of this effect we have also included in the database some parameters describing the plasma edge properties, such as the electron and ion density and temperature, the neoclassical collisionality, the ELM frequency and amplitude. The kinetic quantities have been obtained by using the LIDAR (core and edge) diagnostic and by taking edge density (from the interferometer) and the electron temperature (from the electron cyclotron) at one fixed radius on the top of the pressure pedestal. Moreover, all the “edge parameters” have been obtained by volume averaging between the normalised plasma radii $0.8 < \rho < 0.95$. The edge neoclassical collisionality shows a large variation in the

database ($0.05 < \nu_{\text{edge}}^* < 0.8$), where the higher collisionality has mainly been obtained in experiments at low toroidal magnetic field. In Fig.7 we show the central ion temperature versus ν_{edge}^* . There is a strong decrease of $T_i(0)$ as the collisionality increases. A similar dependence is observable for the central electron temperature. Moreover both the species temperatures show the same behaviour with the edge density, but not with the edge pressure. A linear correlation is also observable between the edge and the central ion temperature ($T_i(0) \sim 3 T_i(\text{edge})$) for all the discharges not presenting the improved central confinement. A more detailed comparison, among the three discharges previously introduced, shows that the two discharges with lower central density also have the same edge density, but this is around a factor four lower than that of Pulse No: 62459 ($n_e(\text{edge}) \sim 4^0 \times 10^{19} \text{ m}^{-3}$). The edge collisionality has the same dependence, being less than 0.1 for discharges Pulse No's: 59137 and 60933, and of the order of 0.2 for Pulse No: 62459. The edge electron temperature is more or less constant among the three discharges, but $T_i(\text{edge})$ is larger for the two pulses at lower density. Finally the plasma pressure is larger for the experiment at higher electron density and, again, similar for the other two.

REFERENCES

- [1]. Challis C.D. Plasma Phys. Control. Fusion **46** (2004) B23.
- [2]. Luce T.C., et al., Phys. Plasmas **11** (2004) 2627.
- [3]. Isayama, A., et al., Nuclear Fusion, **41**, 2001, 761.
- [4]. Isayama, A., "Steady state High-beta Experiments in JT-60U Hybrid Experiments", presented at the ITPA meeting, Naka March 2004.
- [5]. Connors, J.W., et al., "Nucl. Fusion" **44** (2004) R1-R49
- [6]. Joffrin E., Sips A.C.C., Artaud J. F., et al., Nucl. Fusion **45** 626-634
- [7]. Staebler, A., Sips A.C.C., et al., Nucl. Fusion **45** 617-62
- [8]. Maggi et al., this conference
- [9]. Buratti, P., Alper B., Annibaldi S. V., Plasma Phys. Control. Fusion **48** 1005-1018.
- [10]. Joffrin, E., et al., Plasma Phys. Control. Fusion **44** 1203-1214
- [11]. Gormezano, C., et al., Plasma Phys. Control. Fusion **46** B435-B4
- [12]. G. Tresset et al., Proceedings of the 28th EPS Conference on Contr. Fus. And Plasma Phys., Madeira, 2001
- [13]. Crombe K., et al., Phys Rev Lett **95** (2005) 155003-1
- [14]. Tardini G., et al., Proc 31st EPS Conference on Plasma Physics (London, 2004) vol 28G P-4.123.

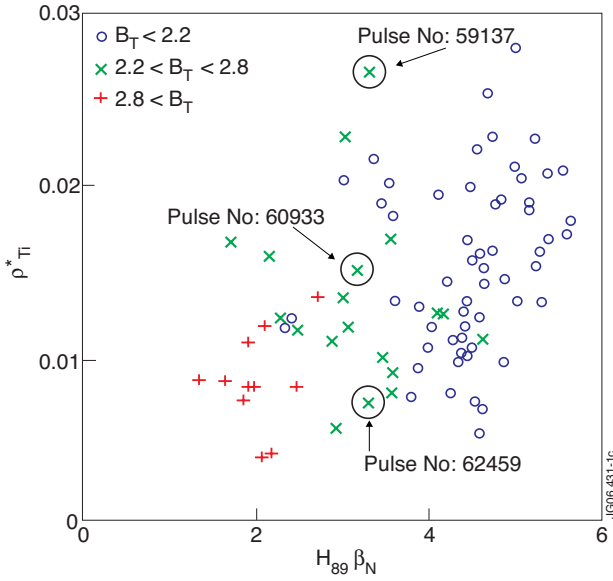


Figure 1: The radial maximum of the ion normalised radius ρ_{Ti}^* is plotted versus the merit parameter $H_{89} \leq \beta_N$ for the database points selected with the criterion that the maximum is inside the plasma region $3.2 < R < 3.55m$. The data are separated for three ranges of toroidal field $B_T(T)$.

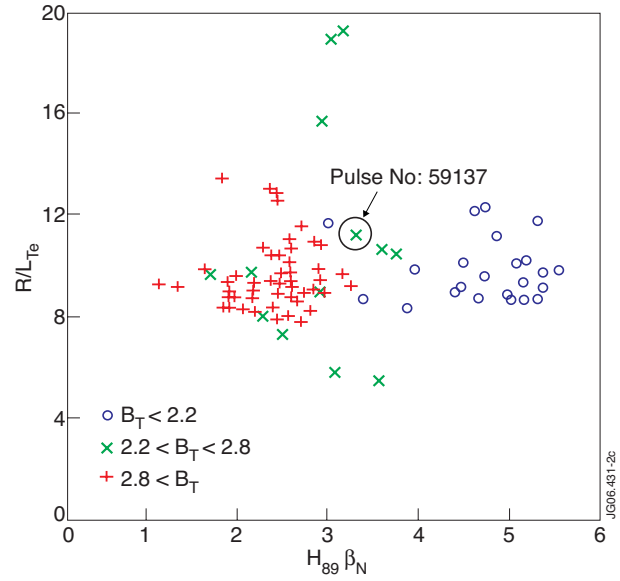


Figure 2: The radial maximum of the inverse of the normalised electron temperature gradient R/L_{Te} is plotted versus the merit parameter $H_{89} \leq \beta_N$ for the database points selected with the criterion that the maximum is inside the plasma region $3.2 < R < 3.55m$. The data are separated for three ranges of toroidal field $B_T(T)$.

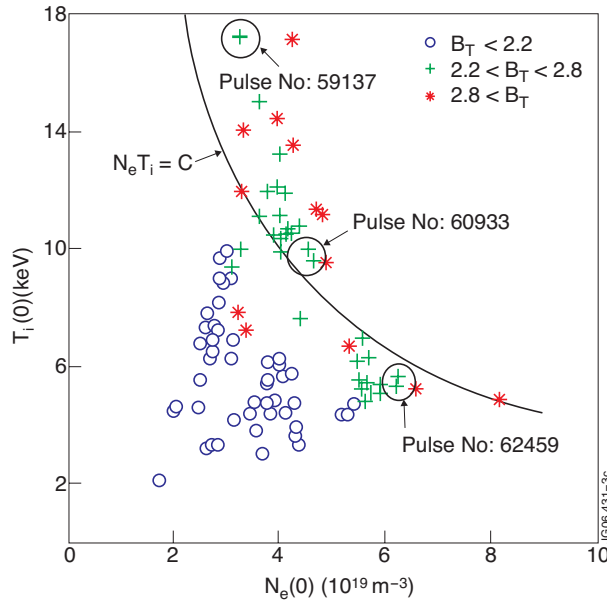


Figure 3: The central ion temperature $T_i(0)$ is plotted versus the central electron density $N_e(0)$ for the database points. The data are separated for three ranges of toroidal field $B_T(T)$. Three discharges similar in any operational parameter, except the density, are shown for comparison. The line represents the constant pressure behavior.

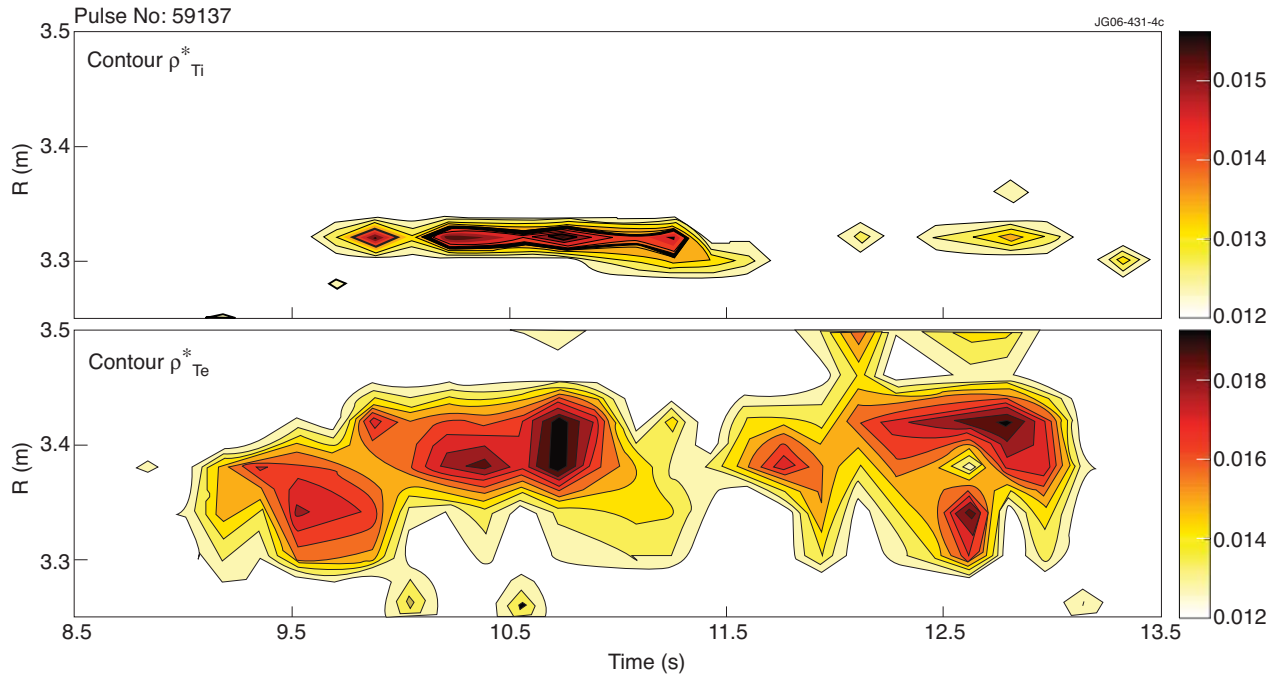


Figure 4: (a)-(b) Pulse No: 59137. The normalized electrons (a) and ions (b) Larmor plasma radius equicontour versus time.

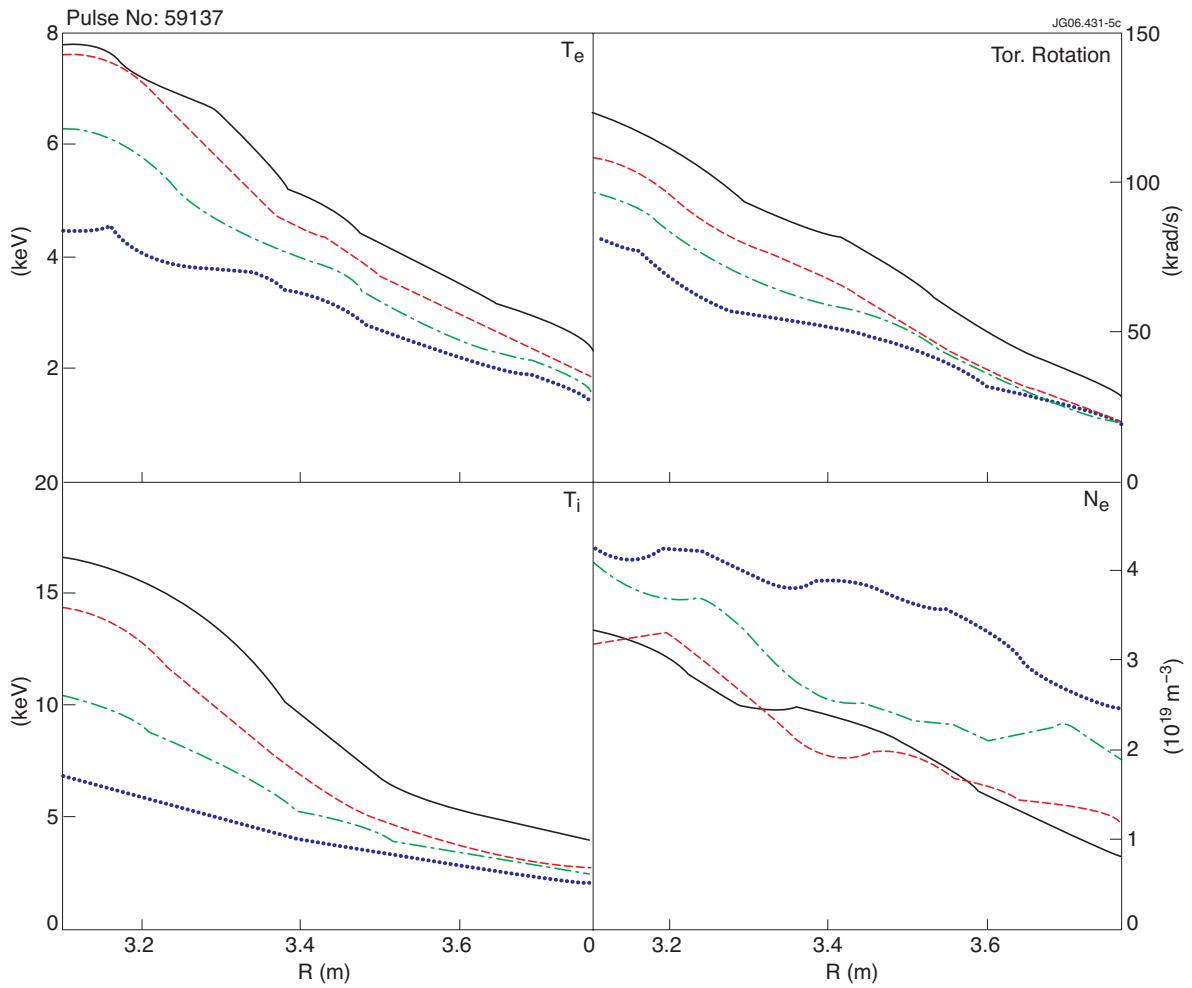


Figure 5: Radial profile of the electron and ion temperature, of the toroidal rotation at four fixed times for the Pulse No: 59137. dotted $t=8.4s$; dot dashed $t=8.9s$; dashed $t=10.1s$; solid $t=11.9s$

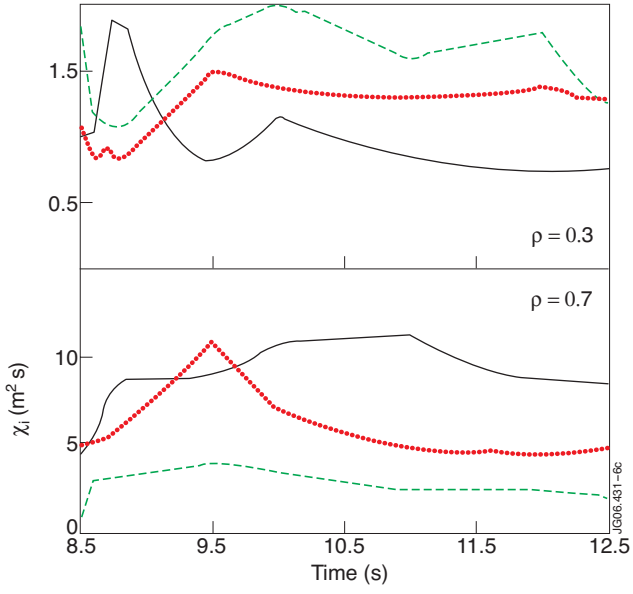


Figure 6: Heat diffusion coefficient versus time at two normalised radii for the three compared Pulse No's: 59137 (black line); 60933 (red dots); 62459 (green dashes).

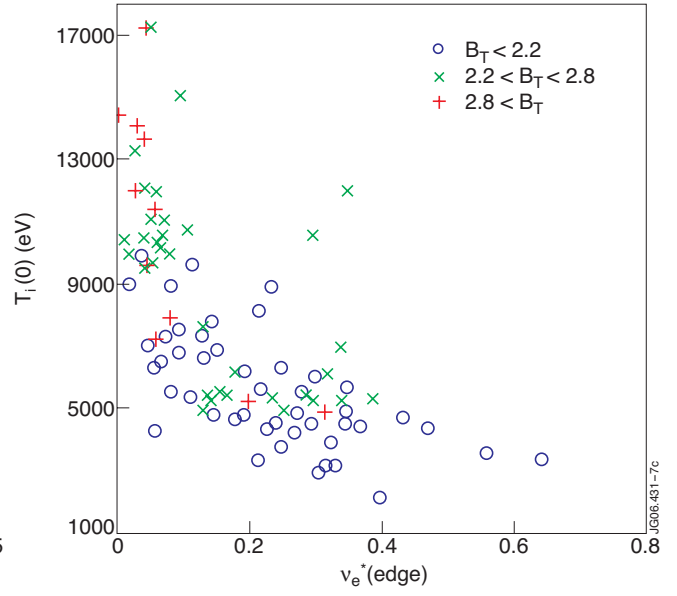


Figure 7: Central ion temperature versus the neoclassical edge collisionality for the database points, the data are selected for three ranges of toroidal field.